Chapter 7

Atmospheric Neutrino Oscillation Search

7.1 Introduction

Atmospheric neutrinos can be detected using different methods. Each method can give informations on the neutrino flux with a particular (detector dependent) energy distribution. Contained and partially contained neutrino events involve mainly neutrinos in the $1-10\ GeV$ energy range, while upward going muons are induced in interactions in the surrounding rock by neutrino with energy of the order of 100 GeV. This implies that oscillation searches using contained or partially contained atmospheric neutrinos present different systematic effects with respect to the search with Long Baseline accelerator neutrinos. Due to the steeply decreasing spectrum, the energy of the bulk of atmospheric contained events will be significantly lower than accelerator one.

Measuring the incoming neutrino zenith angle θ, it is possible to evaluate the travel length L from the production point to the detector. Downward going atmospheric neutrinos travel an average distance L of a few ten of kilometers, mainly in the atmosphere, while neutrinos produced in the bottom hemisphere with respect to the detector location (upward going) travel a maximum distance L equal to the Earth diameter through the Earth volume. The transition probability depends only on the neutrino path length and energy.

In this chapter the results of the calculation of the atmospheric ν_μ and ν_e events which can be detected by the N^OE apparatus will be presented. The N^OE analysis will be performed on two independent data samples. Al

lower energies (contained and partially contained events) a separation between CC ν_μ and ν_e interactions is performed both calorimetrically (chap. 5) and through the recognition of the muon decay (sec. 7.4). In this case, the ratio $R = \frac{\nu_e+\overline{\nu}_e}{\nu_\mu+\overline{\nu}_\mu}$ is evaluated and compared with expectation. At higher energies (upward going stopping and throughgoing muons) the sensitivity to ν_μ oscillation rely on the measurement on the ratio $R' = \mu\ stop/\mu\ through$ [1] which, belonging to different energy ranges (see Fig. 1.1), are differently affected by oscillation.

In the next section, the Montecarlo tools which have been used (atmospheric neutrino flux, neutrino cross section and the simulation software) will presented. Using those simulation tools, the number of ν_μ and ν_e visible interactions in a 4 $kton$ apparatus central detector have been evaluated, separated in contained and partially contained events. Then, the results for upward throughgoing and stopping muons induced by neutrino interactions in the rock surrounding the detector are shown. Finally, the possible implications on the limits on the $(\Delta m^2, sin^2 2\theta)$ oscillation parameter space which $N^O E$ detector can set with atmospheric neutrinos are discussed.

7.2 The atmospheric neutrinos flux

There exist at least four calculations [2, 3, 4, 5] of the flux of atmospheric neutrinos which have been used in the past to interpret the measurements of interactions of $\nu_e(\overline{\nu}_e)$ and $\nu_\mu(\overline{\nu}_\mu)$ in large, deep underground detectors. Possible errors associated with different ν fluxes arise mainly from uncertainties in the input data (15% in the absolute intensity of the primary component and 15% in the evaluation of meson yields). All four calculations agree within a range of 5% for the flavor ratio of neutrinos with $0.4 \leq E_\nu \leq 1\ GeV$ [6], but larger differences exist among the results for normalization and shape of the spectra, and these lead to ambiguities in the interpretation of the measured experimental results. A high normalization that agrees with the observed electron flux favors oscillations predominantly in the $\nu_\mu \leftrightarrow \nu_\tau$ sector.

At low energy, the flux of atmospheric neutrinos is affected by the geomagnetic field, the epoch of the solar cycle and the muon polarization effect. For the Gran Sasso laboratory latitude there is a little suppression of downward going neutrinos due to the geomagnetic field, while the low energy upgoing neutrinos flux (produced in the backward hemisphere) is largely reduced.

The atmospheric neutrino flux calculation of the Bartol group [3] which was used take explicitly into account the effects of the geomagnetic field, of

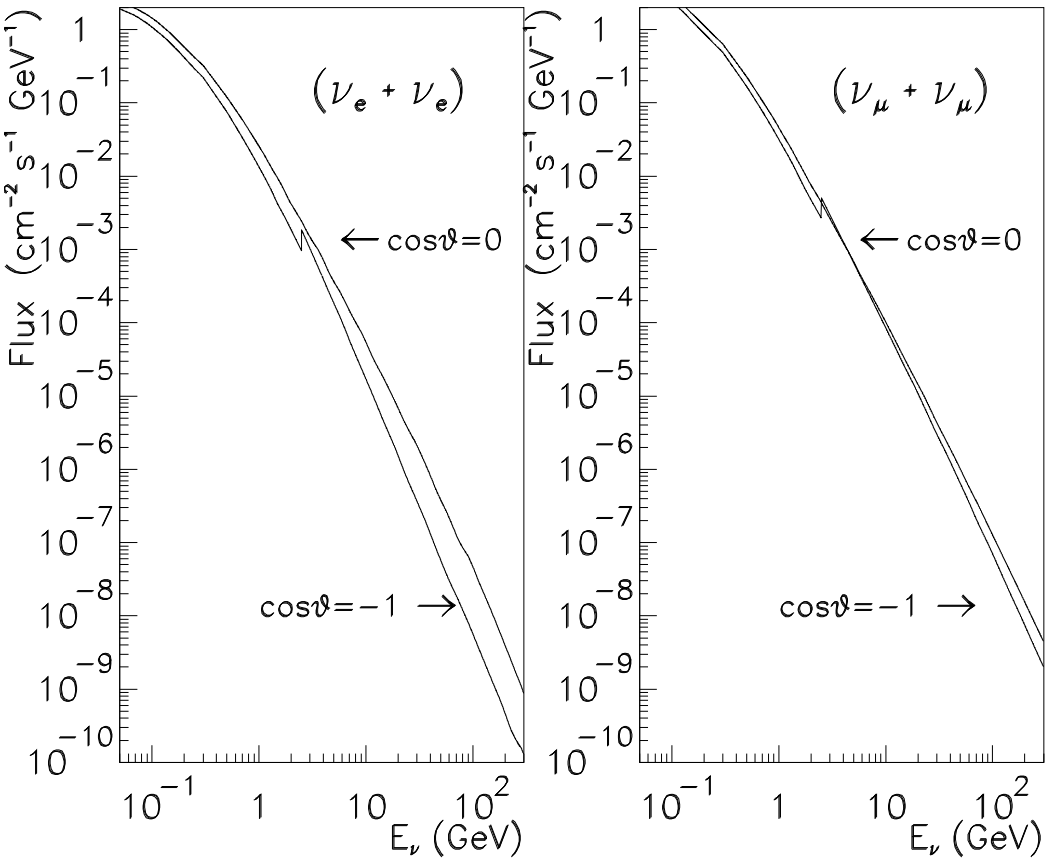

Figure 7.1: The atmospheric neutrino flux as a function of energy and for two values of the zenith angle θ ($cos\theta = 0$ horizontal; $cos\theta = -1$ upward going neutrinos). a) electron neutrinos and antineutrinos; b) muon neutrinos and antineutrinos.

solar modulation and muon polarization. The low energy part of the neutrino spectrum (up to $E_\nu = 2.5\ GeV$) is given in a differential way both in energy, zenith angle and neutrino type for the northern Italy geomagnetic location (negligible difference with Gran Sasso). The high energy part of the spectrum ($E_\nu > 2.5\ GeV$) was also provided by the Bartol group [7]. In Fig. 7.1 the resulting differential flux as a function of E_ν for two different incident angle of $(\nu_\mu + \overline{\nu}_\mu)$ and $(\nu_e + \overline{\nu}_e)$ is presented. The low energy region was evaluated using a value of 0.5 for the phase k of the solar cycle. A small mismatch between the two sets of curves is present.

7.3 The neutrino cross section

In the GeV range (contained and partially contained neutrino events) the neutrino cross section is an important source of systematic uncertainty [8]. For example at $E_\nu = 2\ GeV$ the quasi-elastic $\nu(\overline{\nu})$ scattering cross sections used by the Frejus experiment is $\sim$ 12% (6%) smaller than the one used by Kamiokande, because of different choices of the parameterization of the nucleon form factor.

The neutral current (NC) cross section on nucleon is flavor-independent and also differences on charged current (CC) interaction involving muon and electron (anti)neutrinos are small. The uncertainties on neutrino cross section have therefore a small influence on quantities involving the ratio between two flavors, like $R = \frac{\nu_e+\overline{\nu}_e}{\nu_\mu+\overline{\nu}_\mu}$, in the same energy range. When considering absolute quantities, or their energy dependence the cross section uncertainties do not cancel. Moreover in neutrino interactions with bound nucleon, nuclear effects must be taken into account in addition to the kinematics of the reaction on free nucleon.

A Montecarlo technique which takes into account all these effects and optimized to calculate total and partial channel cross section and the kinematics of the particles in the final state has been used to reproduce neutrino interactions inside the N^OE detector. A similar method was already developed by the Kamiokande experiment [9]. The details of such a Montecarlo are described elsewhere [10]; here only some basic features are presented. CC neutrino cross section was obtained considering separately the contributions of the exclusive channels of lowest multiplicity, i.e. quasi-elastic scattering and single pion production, and describing the additional channels collectively using the deep inelastic scattering (DIS) formulae. The CC neutrino cross section is then the sum of three contributions:

$$\sigma^{CC}_{\nu(\overline{\nu})} = \sigma_{QEL} + \sigma_{1\pi} + \sigma_{DIS} \tag{7.1}$$

The NC cross section can also be decomposed in similar way, with the elastic cross section (that in practice is not observable) replacing the quasi-elastic process.

The CC cross section is well measured [11] only for neutrino energies $E_\nu > 20\ GeV$. At these energies the theory is also solid, the well established formulae of DIS that are valid in the limit of large Q^2 and large W^2 (W is the mass of the hadronic system in the final state) are applicable over most of the phase space, and the cross section can be calculated accurately. Fig. 7.2 shows the neutrino CC cross section and its components used in this

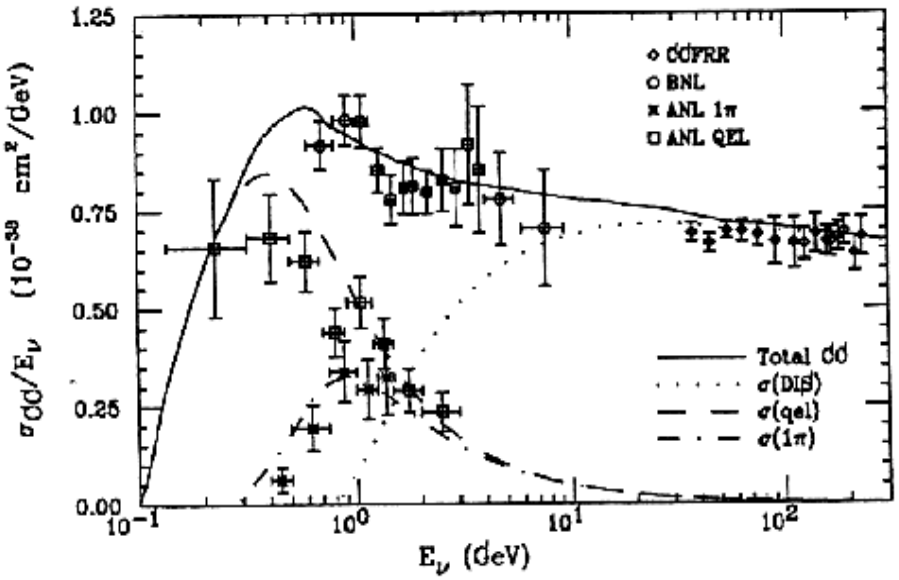

Figure 7.2: The ν_μ CC cross section as sum of the three contributions of (7.1).

work, compared with large statistics data [11]. The effects of nucleon Fermi motion, binding energy, Pauli blocking of the recoil nucleon are taken into account. All these nuclear effects modify the final state kinematics and the cross section of interaction of neutrinos on nucleon.

7.4 Contained and partially contained ν interaction rates in N^OE

To evaluate the neutrino interaction rate in the apparatus, a GEANT- based Montecarlo simulation is used [12]. The tracking of the particles in the final state of the (anti)neutrinos NC and CC interactions through the detector has been carried out and the position, the time, the energy loss and the

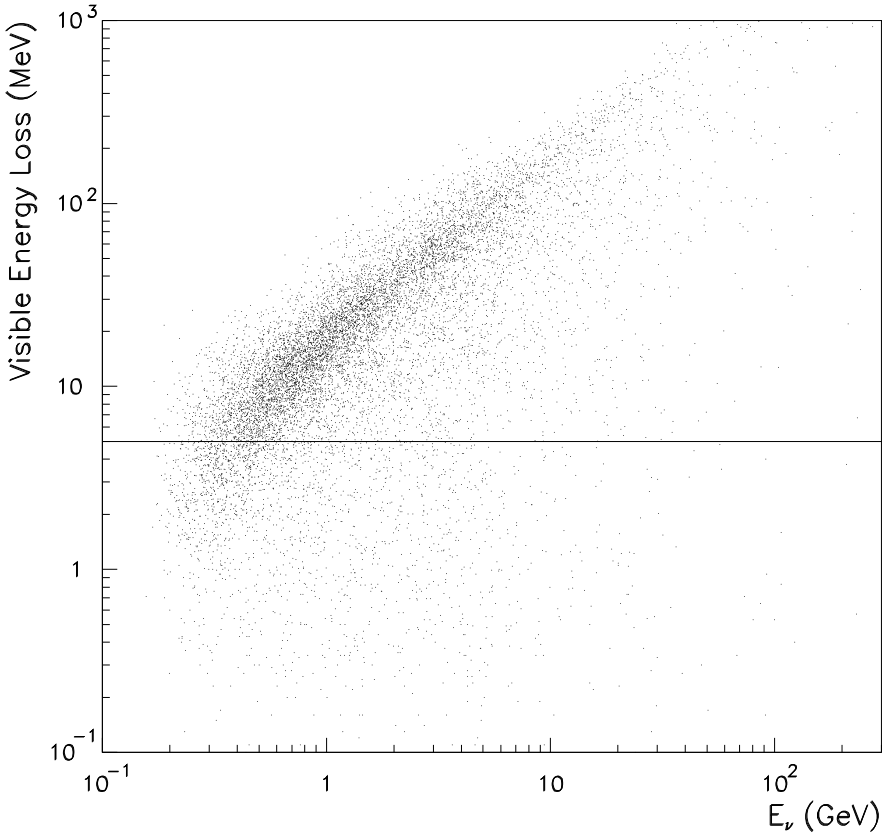

Figure 7.3: Distribution of the total visible energy loss in the scintillator fibers (MeV) versus the incoming neutrino energy (GeV). The horizontal line at 5 MeV indicate the condition of $TR1$ (see text); $\sim$ 30% of neutrino interactions (mostly below 600 MeV) lie below this line.

momentum loss for each particle in any active part of the apparatus were used in the analysis. All GEANT physical processes were turned on and the kinematic cuts were all set to $E_{cut} = 300\ KeV$. A full efficiency ($\epsilon = 1$) and linearity for the detector response is assumed.

Fig. 7.3 shows the distribution of the total visible energy loss in the scintillator fibers for particle in the final state versus the incoming neutrino energy. A neutrino interaction is supposed to trigger the apparatus if the final state satisfy the following two conditions $TR1$ and $TR2$:

i) TR1= $\sum_{i=1,n_{HITS}}(\Delta E)_i > E_{TR} = 5\ MeV$

where n_{HITS} = number of hits in the scintillator fibers and ΔE_i is the visible energy loss in each fiber.

N_{ν_e}	74.4	$(kton \cdot year)^{-1}$
$N_{\overline{\nu}_e}$	22.4	$(kton \cdot year)^{-1}$
N_{ν_μ}	148.2	$(kton \cdot year)^{-1}$
$N_{\overline{\nu}_\mu}$	53.2	$(kton \cdot year)^{-1}$
Total rate	298.2	$(kton \cdot year)^{-1}$

Table 7.1: Montecarlo evaluated interaction rate $(kton \cdot year)^{-1}$ for atmospheric neutrinos with energy $E > E_{min} = 150 MeV$ for a detector at the Gran Sasso location.

ii) TR2 = more than two hits in the central tracking detector.

These requirements set a threshold of $\sim 300\ MeV$ for the neutrino energy (see Fig. 7.3). For this reason, both the low and high energy neutrino flux discussed above are used; the phase of solar cycle was set to $k = 0.5$ and the minimum energy for the (anti)neutrinos to $E_{min} = 150\ MeV$.

Both electron (anti)neutrino and muon (anti)neutrino interactions were considered. The global interaction rate in the apparatus for each flavor and integrating over the whole $\Delta\Omega = 2\pi$ solid angle, is reported in Table 7.1.

A data sample of 15000 events was generated for a 5 *kton* N^OE total detector mass. This data sample corresponds approximately to 10 y of data taking. To define a detectable interaction the final state must satisfy the requirements defined above. 1155/15000 events do not fired any active detector; 9152/13845 events passed TR1 and 7614/13845 events $TR1 \wedge TR2$.

Each event which *triggered* the apparatus was then classified as totally or partially contained if all visible particles in the final state are contained or not in an inner volume whose limit is 30 cm far from the boundary of the central detector. In Table 7.2 the number of visible event/year for partially and totally contained evens (divided in ν_e and ν_μ CC and NC interactions) for a 4 *kton* central detector mass is presented. The neutrino energy interval giving rise to 90% of the signal (5% of the highest and 5% of the lowest energy events were excluded) is reported below. Finally, the average neutrino energy in the interval is presented.

Fig. 7.4 shows the $(\nu + \overline{\nu})$ interaction yields versus the neutrino energy for partially and totally contained events.

In order to make an oscillation measurement, it is necessary to separate the ν_e from ν_μ CC interactions. The calorimetric methods described in chap. 5 can also be used for atmospheric neutrinos. For partially contained events

	$(\nu_e + \overline{\nu}_e)$ CC	$(\nu_\mu + \overline{\nu}_\mu)$ CC	$(\nu + \overline{\nu})$ NC
Partially contained (y^{-1})	92.2	273.1	62.6
E_ν (90% $C.L.$)(GeV)	$0.5 < E_\nu < 16$	$0.6 < E_\nu < 35$	$0.8 < E_\nu < 40$
$< E_\nu > (GeV)$	3.1	5.4	6.8
Totally contained (y^{-1})	108.6	174.0	46.3
E_ν (90% $C.L.$)(GeV)	$0.4 < E_\nu < 6$	$0.4 < E_\nu < 4$	$0.6 < E_\nu < 15$
$< E_\nu >$ (GeV)	1.5	1.2	3.2

Table 7.2: Number of partially and totally contained neutrino interactions for a 4 $kton$ central detector for one year of live time. The sample was divided in ν_e and ν_μ CC interactions. The neutrino energy interval giving rise to 90% of *triggering* events are also reported with the average value $< E_\nu >$ of the neutrino energy in that interval.

the lepton energy is large enough to allow a calorimetric measurement of the lepton flavor. However when the lepton energy is less than $\sim 500\ MeV$ the separation between the two flavors is difficult. In this case it might be possible to separate ν_e from ν_μ interactions by detecting the electron from the muon decay using the timing capability of the $N^{O}E$ apparatus.

This possibility has been studied using the totally contained ν_μ interactions data sample. In Table 7.3 it is given the fraction of this data sample in which the muon decay ($\mu \to e\nu_e\nu_\mu$) happens with a delay Δt from the ν_μ primary interaction, assuming that the μ^- have $\sim 55\%$ probability of forming a μ mesic atom in the radiator.

For instance, 40.5% of the muon decay can be detected (after a primary trigger in a BCE element with a threshold energy $E_p > 5\ MeV$) if a delayed detection is performed in the same element (and the neighboring) with $\Delta t > 100\ ns$ and a lower threshold energy $E_s = 1\ MeV$.

Fig. 7.5 shows the distribution of the energy released in the scintillator fibers by electrons from muon decay with $\Delta t > 100\ ns$.

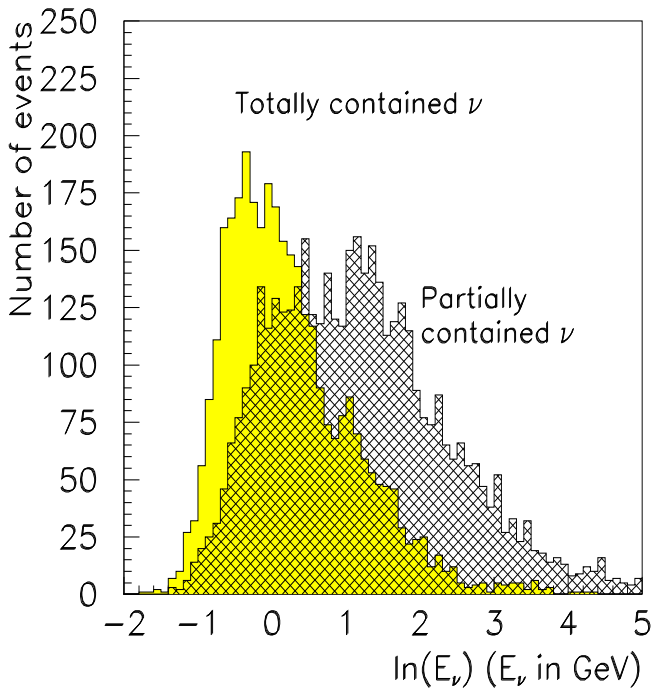

Figure 7.4: Energy distribution of simulated atmospheric ν_μ and ν_e giving rise to partially and totally contained events detected with the N^OE apparatus. Units for the vertical axis refers to a 4 *kton* detector and $\sim$ 10 *y* of data taking.

7.5 Upward throughgoing and stopping muons

7.5.1 The simulation for upward going muons

The extremely good timing capability of the N^OE detector can allow a precise determination of the versus of the track, even for relatively short tracks. For the evaluation of the upward throughgoing and stopping muons induced by neutrino interactions in the rock surrounding the apparatus a method slightly different than that used for contained interactions has been adopted. This mainly to save CPU time on simulation and because the neutrino cross section in this energy range is more firmly established. A differential flux of muons

ν_μ $(Tot.Cont.)$	100%	$\Delta E^e_{Vis} > 1MeV$	$\Delta E^e_{Vis} > 2MeV$
$\mu \to e$ $(\Delta t > 0)$	60.5	42.2	24.3
$\Delta t > 50$ ns	58.4	42.0	24.0
$\Delta t > 100$ ns	56.3	40.5	23.2
$\Delta t > 200$ ns	52.9	37.9	21.9

Table 7.3: Percentage fraction of totally contained ν_μ CC interaction with a visible muon decay. In the first column the number of muon decaying with a delay time Δt from the neutrino interaction ($t = 0$) greater than $0, 50, 100$ and 200 ns and with $\Delta E^e_{Vis} > 0$. In the second and third, the fraction of case in which ΔE^e_{Vis} is greater than 1, 2 MeV. ΔE^e_{Vis} is the visible energy loss in the scintillator fibers for the electron from the muon decay.

with zenith angle θ and energy $E > E_\mu$ at the detector from atmospheric neutrino has been evaluated as:

$$N_\mu(E > E_\mu) = \sum_{\nu_\mu, \overline{\nu}_\mu} \int dE'_\mu \int dE_\nu \cdot R(E_\mu, E'_\mu) \cdot \frac{d\sigma_{\nu\overline{\nu}}}{dE'_\mu} \cdot \Phi(E_\nu, \theta) \qquad (7.2)$$

where $\frac{d\sigma_{\nu\overline{\nu}}}{dE'_\mu}$ is the charged current cross section for a $\nu(\overline{\nu})$ of energy E_ν to produce a μ of energy E' and $R(E_\mu, E'_\mu)$ is the effective range in rock for the μ to survive with energy $E > E_\mu$. To compare the Montecarlo with data, the detector acceptance and efficiency must be folded with (7.2).

For the neutrino flux, the high energy Bartol code [7] has been used. For this part they estimate the systematic error on the flux of upward-going muons with energy greater than 3 GeV at the detector due to uncertainties in the neutrino flux to be $\pm 13\%$ when constraints from atmospheric muon measurements are taken into account [13]. The cross-sections for neutrino interactions have been calculated using the Morfin and Tung parton distributions set B1-DIS [14]. The systematic error on the expected flux of throughgoing muons due to all uncertainties in the cross section is of the order of $\pm 7\%$. The propagation of muons to the detector has been done using the energy loss calculation of Lohmann et al. [15] in standard rock. Due to the uncertainties on the energy loss, the uncertainties on the muon flux is of the order of $\pm 3\%$. The total systematic uncertainty on the expected flux of muons at the detector is given by adding the errors from the neu-

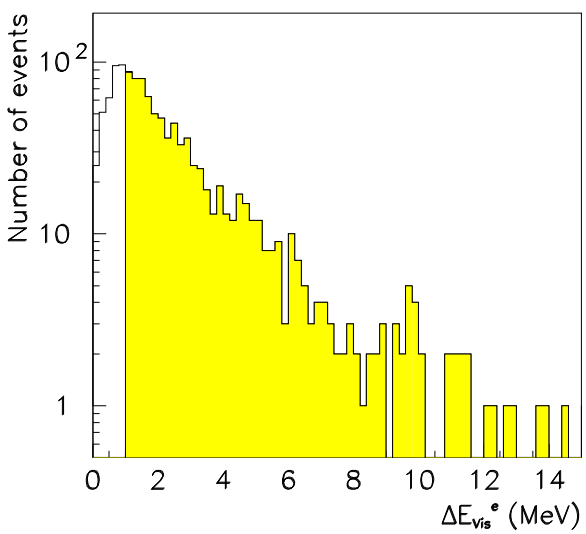

Figure 7.5: Energy loss distribution ΔE^e_{Vis} in the scintillator fibers of the electron (or positron) from muon decay. All electrons with a delay $\Delta t > 100\ ns$ from the primary ν_μ interaction were included. The shaded area refers to $\Delta E^e_{Vis} > 1\ MeV$.

trino flux,cross-section and muon propagation in quadrature. The resulting systematic uncertainty is of the order of $\pm 17\%$.

7.5.2 Simulation results

Using the above neutrino flux, neutrino cross section DIS structure function and energy loss, the number of muons reaching the N^OE detector as a simple box is:

$$R_{\mu^-} = 169.8\ y^{-1}$$
$$R_{\mu^+} = 80.3\ y^{-1}$$
$$R_{tot} = 250.1\ y^{-1}$$

A sample of 10000 events reaching the box, which are equivalent to 40 years of data taking was generated. 6169/10000 events satisfy the trigger requirements $TR1 \wedge TR2$.

THROUGHGOING	110.5 (y^{-1})
$L_T > 1\ m$	95.1 (y^{-1})
STOPPING	43.7 (y^{-1})
$L_T > 5\ cm$	34.7 (y^{-1})

Table 7.4: Rate (y^{-1}) of throughgoing and stopping upward going μ for the N^OE detector. L_T is the length of the longest track in the final state.

Due to the limited N^OE area with respect, for example, to the MACRO detector, the rate of upward going muons is relatively small. However, due to the higher mass/area ratio, the fraction of stopping muons will be significatively greater. The number of throughgoing and stopping muons are reported in Table 7.4, where L_T is the minimum track length in the apparatus. Moreover, the distribution of the ratio between stopping/throughgoing events versus the zenith angle is sensitive to the (E_ν/L) rate in the neutrino oscillations formula.

Finally, the very good granularity and high mass of the apparatus could permit an entirely different approach for oscillation measurement. A fiducial cut in the bottom detector will be necessary to eliminate the background due to upward going pions induced by atmospheric muons passing near the detector. The high density of this apparatus will be of great help in this background reduction. The main idea is to use not only the simple rate between the number of stopping over the number of throughgoing muons to set limits on neutrino oscillations but also the z-coordinate distribution of the end point is sensitive to the neutrino energy spectrum and is affected by neutrino oscillations. Fig. 7.6 shows the number of stopping events versus the N^OE z-coordinate of the track end point. The lower detector edge is $z = -800\ cm$.

7.6 Discussion on neutrino oscillations sensitivity.

In this paragraph a summary of the N^OE sensitivity on neutrino oscillations using atmospheric neutrino data is presented. Only the simpler case of two-flavors neutrino oscillations is discussed without matter effect. In Table 7.5 the expected number of events is presented for all neutrino interactions topol-

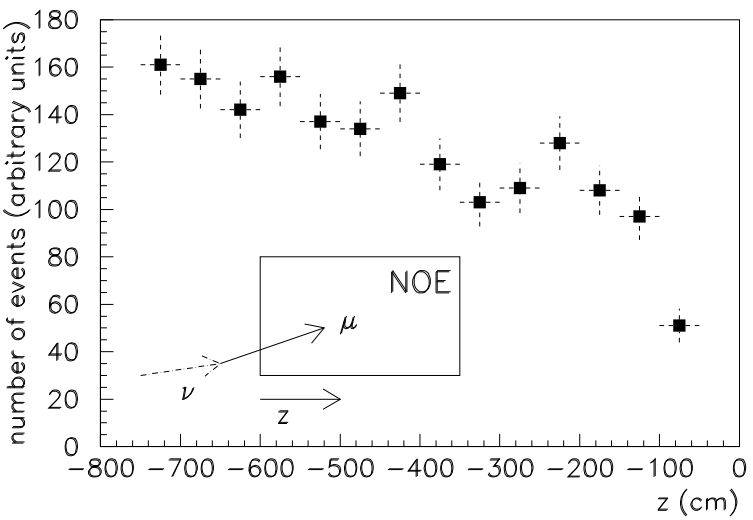

Figure 7.6: z-coordinate distribution of the point in the N^OE detector in which upward going muons from atmospheric neutrino stop. A sketch of the interaction is drawn; the $\nu_\mu \to \mu$ interaction happens in the rock below the apparatus.

ogy discussed above. A running time of three years with 100% duty cycle is assumed.

First, N^OE will detect a number of ν_μ, ν_e CC contained or partially contained events which can provide an absolute measurement of the flux of these neutrinos as a function of energy and zenith angle. The energy range for contained events is around $0.4 < E_\nu < 6\ GeV$ while it is $0.6 < E_\nu < 35\ GeV$ for partially contained events. The ratio $R = \frac{\nu_e + \overline{\nu}_e}{\nu_\mu + \overline{\nu}_\mu}$ from each subsample (i.e. for events in the same energy range) is less affected by systematic uncertainties than the absolute value. Also the dependence of the ratio R on the neutrino energy and zenith angle can be compared with Montecarlo predictions as well as the apparent NC/CC ratio for atmospheric neutrinos integrated over the ν spectra.

Most of this analysis relies on the separation between ν_μ and ν_e interactions wich can be performed using calorimetric methods or using the timing capability of the detector. The Montecarlo results suggest the possibility to reach a separation efficiency of $\sim 60\%$ for totally and $\sim 80\%$ for partially contained events using both the calorimetric and timing methods.

Second, upward throughgoing and stopping events due to neutrino inter-

action in the rock below the apparatus cover a different neutrino energy range (from $\sim 2\ GeV$ up to few hundred GeV). The sensitivity of N^OE reported in Table 7.5 in this energy range has been calculated from the total ratio $R' = \mu\ stop/\mu\ through$. Moreover this ratio can be measured versus the zenith angle. Most upward going muons with energy from few hundred MeV up to 10 GeV will be stopped in the detector. The distribution of stopping events versus the path length in the detector is also dependent on the neutrino energy spectrum. An anomalous distribution will be a signature for oscillations.

In the atmospheric neutrino flux, the contamination of ν_τ is completely negligible. If neutrino oscillations occur through the $\nu_e \leftrightarrow \nu_\tau$ channel, the only detectable effect would be a decrease in the ν_e counting rate in the ratio R.

If oscillations occur via the $\nu_\mu \leftrightarrow \nu_\tau$ channel with $\Delta m^2 > 6\ 10^{-4}$ it would produce a decrease of muon counting rate and a consequent higher value of R with respect to Montecarlo prediction. If $\Delta m^2 > 2\ 10^{-3}$ it would affect also the ratio R' between upward stopping and throughgoing muons.

Finally, if $\nu_e \leftrightarrow \nu_\mu$ transition happens, the values of the ratio $R = \frac{\nu_e + \overline{\nu}_e}{\nu_\mu + \overline{\nu}_\mu}$ and the number of stop/throughgoing upward going events respectively will be affected depending on the value of Δm^2.

The accessible region in the $(\Delta m^2, sin^2 2\theta)$ oscillation parameter space is limited mainly by the error on the measured quantities (statistics+ theoretical uncertainties on flux and cross section) for the $sin^2 2\theta$ variable and by the minimum value of $< E_\nu / L >$ for the Δm^2 variable.

In Table 7.5 a summary of the results which can be achieved with this 3 $year$ run it is reported. It is assumed that $\theta_{min} \sim \Delta N/N$ where N is the number of detected neutrinos and ΔN is the total error (statistical and systematic) in that measurement. The systematic error is around $15 - 20\%$ for absolute measurement and 10% for the ratios.
For Δm^2_{min} it is assumed $\Delta m^2_{min} =< E_\nu > /D/2$ where D is the Earth diameter and $< E_\nu >$ the mean neutrino energy.

	ν_μ CC	ν_e CC	$< E_\nu >$ GeV	E_T GeV	σ (stat)	$\sigma_T \sim \Delta sin^2 2\theta$ (sta+syst)	Δm^2_{min} eV^2
Par.Cont.	820	280	~ 4	0.6	0.08	0.13	6.10^{-4}
Tot.Cont.	520	325	~ 1.3	0.4	0.09	0.14	2.10^{-4}
Stop	100		~ 10	2.	0.10	0.14	2.10^{-3}
Through	330		~ 100	10	0.06	0.12	2.10^{-2}

Table 7.5: Number of events for ν_e and ν_μ CC contained interactions (row 1 and 2) and the number of stopping/throughgoing events for a three years data taking (row 3 and 4). Then, from column 3, the average values of the neutrino energy $< E_\nu >$ are reported; the evaluated minimum energy E_T for a neutrino giving rise to an observable event in each category; the statistical error (percent, 90% $C.L.$); the total error (percent, 90% $C.L.$); for all the theoretical uncertainties on the ratios $R = \frac{\nu_e+\overline{\nu}_e}{\nu_\mu+\overline{\nu}_\mu}$ and $R' = stop/throughgoing$ a value of 10% is assumed; the value of the $< E_\nu > /D/2 = \Delta m^2_{min}$.

Bibliography

[1] W.Frati et al., Phys. Rev. D48 (1993) 1140

[2] E.V.Bugaev and V.A.Naumov, Phys. Lett. B232(1989) 391

[3] G.Barr, T.K.Gaisser and T.Stanev, Phys. Rev. D39(1989) 3532

[4] M.Honda, K.Kasahara, K.Hidaka and S.Midorikawa, Phys. Lett. B248 (1990) 193

[5] H.Lee and Y.S.Koh, Nuovo Cimento B105 (1990) 883

[6] T.K.Gaisser, Phil. Trans. Roy. Soc. Lond. A346 (1994) 75

[7] V.Agrawal, T.K.Gaisser, P.Lipari and T.Stanev, (1993) unpublished

[8] P.Lipari et al., Phys. Rev. Lett. 74 (1995) 4384

[9] N.Nakahata et al., J. Phys. Soc. Jpn. 55 (1986) 3786

[10] P.Lipari, M.Lusignoli and F.Sartogo, Phys. Lett. 74 (1995) 4384

[11] Rev. Particle Properties, Phys. Rev. D45, part II (1992)

[12] R.Brun et al., CERN Report DD/EE84-1, 1987

[13] T.K.Gaisser, private communication

[14] J.G.Morfin and W.K.Tung, Z.Phys. C52 (1991) 13

[15] W.Lohmann et al., CERN-EP/85-03, March 1985